Ratio $|g_A/g_V|$ derived from the proton spectrum in free-neutron decay

Chr. Stratowa, R. Dobrozemsky, and P. Weinzierl

Physics Institute, Research Center Seibersdorf, Österreichische Studiengesellschaft für Atomenergie m.b.H., Lenaugasse 10, A-1082 Vienna, Austria

(Received 11 July 1978)

The electron-neutrino angular-correlation coefficient was determined by measuring the shape of the proton recoil spectrum from free-neutron decay. The protons leaving a highly evacuated tangential reactor beam tube were analyzed by a spherical condenser spectrometer and counted in an ion-electron converter detector. The design of the apparatus, the possible disturbing influences, and the measures to reduce their effects are discussed. The remaining corrections were either calculated or determined by auxiliary measurements and applied to the spectral shape. The sources of systematic errors are considered and included in the final results. We obtained $a = -0.1017 \pm 0.0051$ giving $|g_A/g_V| = 1.259 \pm 0.017$.

I. INTRODUCTION

It is well known that studies on nuclear β decay allow testing the predictions of various forms of weak-interaction theory. An investigation of the decay of the free neutron avoids possible complications from nuclear structure. The decay probability per unit time, as given, e.g., by Jackson *et al.*,[1] has the general form (setting $c = \hbar = 1$)

$$P(E_e, \vec{p}_e, \vec{p}_{\bar{\nu}}) = F(E_e)\left[1 + a\frac{\vec{p}_e \cdot \vec{p}_{\bar{\nu}}}{E_e E_{\bar{\nu}}} + A\frac{\vec{\sigma} \cdot \vec{p}_e}{E_e} + B\frac{\vec{\sigma} \circ \vec{p}_{\bar{\nu}}}{E_{\bar{\nu}}} + D\frac{\vec{\sigma} \circ (\vec{p}_e \times \vec{p}_{\bar{\nu}})}{E_e E_{\bar{\nu}}}\right], \tag{1}$$

with $\vec{p}_e$ and $\vec{p}_{\bar{\nu}}$ the momentum of electron and antineutrino, respectively, and $\vec{\sigma}$ the polarization of the decaying neutron. E_e is the electron energy, $F(E_e)$ the Fermi function and a, A, B, and D are the coefficients of asymmetry. The parameters a, A, B, and D depend on the form of coupling. As experiments have shown, the weak interaction can be described by a $V-A$ theory yielding a maximum of parity violation. Writing for the ratio of coupling constants

$$g_A/g_V = \lambda = |\lambda| e^{i\phi}, \tag{1a}$$

we get the asymmetry coefficients as

$$a = \frac{1-|\lambda|^2}{1+3|\lambda|^2}, \quad A = -2\frac{|\lambda|^2 + \mathrm{Re}\lambda}{1+3|\lambda|^2},$$

$$B = 2\frac{|\lambda|^2 - \mathrm{Re}\lambda}{1+3|\lambda|^2}, \quad D = 2\frac{\mathrm{Im}\lambda}{1+3|\lambda|^2}. \tag{1b}$$

Evidently, a knowledge of A and B determines λ completely; a measurement of a gives the absolute value of λ. A value $D \neq 0$ would imply a violation of time reversal. The vector coupling constant g_V can be obtained from pure Fermi transitions ($0^+ \rightarrow 0^+$ transitions). Raman *et al.*[2] quote the best presently known value of $g_V = (1.3965 \pm 0.0010) \times 10^{-49}$ erg cm^3. On the other hand, it is not possible to obtain the axial-vector coupling constant g_A from pure Gamow-Teller transitions directly. The most precise measurements of A, B, D, and a, together with the respective values of λ are compiled in Tables I and II. For $D = 0$ one gets $\phi = 0$ or π; the values of A and B show that the sign of λ is negative. The first three measurements quoted in Table II implied a coincident observation of electrons and protons. The last quoted data refer to a preliminary result of a measurement of the recoil proton spectrum obtained at the Research Center Seibersdorf. A detailed discussion of this statistically more favorable method and of the final results are presented here.

II. MEASUREMENT OF THE ANGULAR-CORRELATION COEFFICIENT a BASED ON THE ENERGY SPECTRUM OF THE RECOIL PROTONS

For unpolarized neutrons ($\langle\vec{\sigma}\rangle = 0$) Eq. (1) simplifies to

$$P(E_e, \theta) = F(E_e)\left(1 + a\frac{p_e}{E_e}\cos\theta\right), \tag{2}$$

with θ the angle between electron and antineutrino. Calculating the proton recoil energy T and the angle ϕ between proton and electron, Kofoed-Hansen[20] obtained $P(E_e, T)$, $P(E_e, \phi)$, and $P(T, \phi)$. Following a suggestion of Riehs,[21] we decided to measure the energy spectrum of the recoil protons, which corresponds to an integration of $P(E_e, T)$ over all electron energies. Nachtmann[22] calculated the spectral shape $N(T)$ of the proton distribution in the limit of nonrelativistic nucleon

TABLE I. Measured values of A, B, and D and corresponding λ values from polarized neutron decay.

Reference	A	B	D	λ
Clark and Robson, 1960–1961 (3,4)	−0.09 ±0.05	+0.96 ±0.40	−0.14 ±0.20	−1.20 ±0.12
Burgy *et al.*, 1960 (5)	−0.114±0.019	+0.88 ±0.15	+0.04 ±0.05	−1.25 ±0.05
Christensen *et al.*, 1969–1970 (6,7)	−0.115±0.008	+1.01 ±0.04	•••	−1.26 ±0.02
Erozolimskii *et al.*, 1970–1971 (8,9,10)	−0.118±0.010	+0.995±0.034	−0.01 ±0.01	−1.27 ±0.025
Erozolimskii *et al.*, 1974 (11)	•••	•••	−0.0027±0.0033	•••
Steinberg *et al.*, 1974–1976 (12,13)	•••	•••	−0.0011±0.0017	•••
Krohn and Ringo, 1975 (14)	−0.113±0.006	•••	•••	−1.258±0.015
Erozolimskii *et al.*, 1977 (15)	−0.115±0.006	•••	•••	−1.263±0.015

energies

$$N(T)=\frac{g_V^2 m_n}{4\pi^3}\frac{1}{1+3a}\left\{\int_{E_e(1)}^{E_e(2)} F(E_e-m_e)[4(\Delta-E_e)E_e]\,dE_e + a\int_{E_e(1)}^{E_e(2)} F(E_e-m_e)[4(\Delta-E_e)E_e-2(\Delta^2-m_e^2)+4m_nT]\,dE_e\right\}, \tag{3}$$

with

$$E_e^{(1,2)}=\frac{\Delta[1-m_e/\Delta\mp(2m_nT)^{1/2}/\Delta]^2}{2[1\mp(2m_nT)^{1/2}/\Delta]}, \tag{3a}$$

$\Delta=m_n-m_p$ stands for the total energy of the neutron decay.

III. EXPERIMENTAL SETUP

The aim of the design of the apparatus was to keep every known disturbing influence on the intensity of the spectrum measured below 0.1%. The apparatus is shown in Fig. 1. The source consists of the neutrons decaying in a tangential through tube of the ASTRA reactor. One end of the beam tube leads into the spectrometer and detector system while the other end carries a proton source for reference purposes. Protons with $T_{max}=751.4$ eV are emitted from the decaying neutrons. The small solid angle defined by the apertures at z_1 and at z_2 select the protons for the energy spectrometer (90° spherical condenser). The particles passing the exit aperture of the condenser are accelerated to an energy of 25 keV and focused onto a thin Al foil. The electrons ejected from both sides of this foil are accelerated and focused onto two plastic scintillators and are counted in coincidence. This counting principle, first described by Kraus and White,[23] gives a low background and sufficient mass discrimination.

The reference proton source is used for energy calibration, for the determination of the resolution function, for detector adjustment, and for other experimental checks. As already mentioned, the essential condition to be met in this measurement is to leave the spectral shape of the decay protons undisturbed, because the angular-correlation coefficient a is strongly dependent on this shape. Therefore, all disturbing influences (electric and magnetic fields, residual gas scattering, proton-energy dependent focussing conditions, energy calibration errors due to the potential distribution in the reference proton source, etc.) have to be studied carefully and either eliminated by technical measures or corrected for on the basis of additional measurements or reliable calculations. The apparatus in all its parts and functions must be considered from this point of view.

TABLE II. Measured values of a and corresponding λ values from unpolarized neutron decay.

Reference	a	$\lvert\lambda\rvert$
Trebukhovskii *et al.*, 1959 (16)	−0.06 ±0.13	1.14 ±0.34
Vladimirskii *et al.*, 1961 (17)	−0.12 ±0.04	1.32 ±0.15
Grigor'ev *et al.*, 1967 (18)	−0.091±0.039	1.22 ±0.12
Dobrozemsky *et al.*, 1975 (19)	−0.099±0.011	1.250±0.036

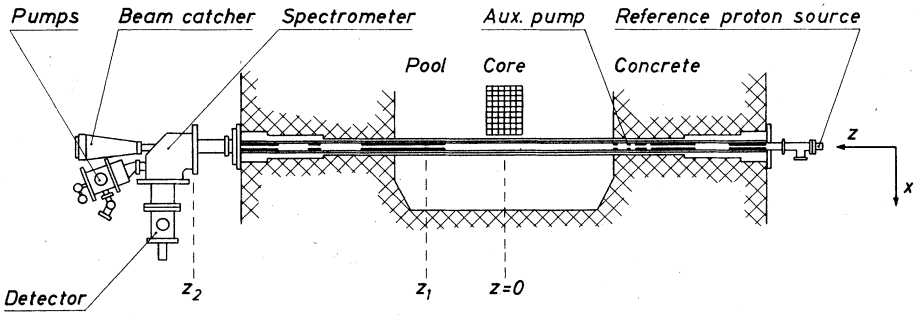

FIG. 1. Experimental setup.

A. The source of decay protons

Figure 2 shows the thermal-neutron flux density, $\Phi_{th}(z)$, and the z component of the thermal-neutron current density, $J_z(z)$, as obtained by Au- and Cd-foil activation technique (see Ref. 24). The maximum of the thermal-neutron flux at 7 MW reactor power amounts to $3.56\times10^{12}\ n_{th}/\mathrm{cm}^2\,\mathrm{sec}$. The epithermal- and fast-neutron flux densities are $1.2\times10^{12}\ n_{epi}/\mathrm{cm}^2\,\mathrm{sec}$ and $1.0\times10^{12}\ n_f/\mathrm{cm}^2\,\mathrm{sec}$, respectively. The peak value of the γ dose rate, $D_{\gamma 0}$, amounts to 3.9×10^7 R/h (0.11 W/g). The transverse gradients in the center of the decay source ($z=0$) are

$$\partial\ln(\Phi/\Phi_0)/\partial x = -0.026/\mathrm{cm},$$

$$\partial\ln(\Phi/\Phi_0)/\partial y = 0.016/\mathrm{cm},$$

$$\partial\ln(D_\gamma/D_{\gamma 0})/\partial x = -0.011/\mathrm{cm},$$

$$\partial\ln(D_\gamma/D_{\gamma 0})/\partial y = 0.0067/\mathrm{cm}.$$

According to Christensen *et al.*,[25] the decay constant Λ of the free neutron is 1.09×10^{-3}/sec. The average velocity $\bar{v}$ of the thermal neutrons is 2.7×10^5 cm/sec. The two apertures of 4.0 cm (at $z_1=90$ cm) and of 3.8 cm (at $z_2=387.5$ cm) define the proton rate entering the spectrometer. Neglecting density gradients in the x and y direction, we get a constant area density n_a of decay protons at the aperture at z_1,

$$n_a = \Lambda\int_{-\infty}^{+\infty}\Phi_{th}(z)/\bar{v}\,dz\,. \tag{4}$$

This gives $n_a = 6.98\times10^5$ decay protons/cm^2 sec, and a corresponding proton flux into the spectrometer of 89.4 protons/sec (all values for 7 MW reactor power).

The thermal movement of decaying neutrons adds the momentum $\vec{q}$ of the neutrons before decay to the center-of-mass momentum $\vec{p}'$ of the protons, giving the proton momentum in the laboratory system as $\vec{p}=\vec{p}'+\vec{q}$. Since only protons emitted close to the z direction reach the spectrometer, and since $|\vec{q}|\ll|\vec{p}|$, we can write $p_z = p' + q_z$. For a symmetrical reactor q_z averages out to zero. The general case has been treated by Nachtmann and Paul.[26] Their result, in a simplified form, is

$$\bar{q}_z = m_n J_z/n\,. \tag{5}$$

J_z is equal to $J_z^+ - J_z^-$. Introducing an asymmetry factor in the z direction, A_z (defined as the ratio between neutron current density and neutron flux density), we get $J_z = A_z J_z^+$. The factor A_z is given by

$$A_z = \int_{-\infty}^{+\infty} J_z(z)dz \Big/ \int_{-\infty}^{+\infty}\Phi_{th}(z)\,dz\,. \tag{6}$$

Taking the data from Fig. 2, we obtained $A_z = 0.021\pm0.004$. That way the proton momentum

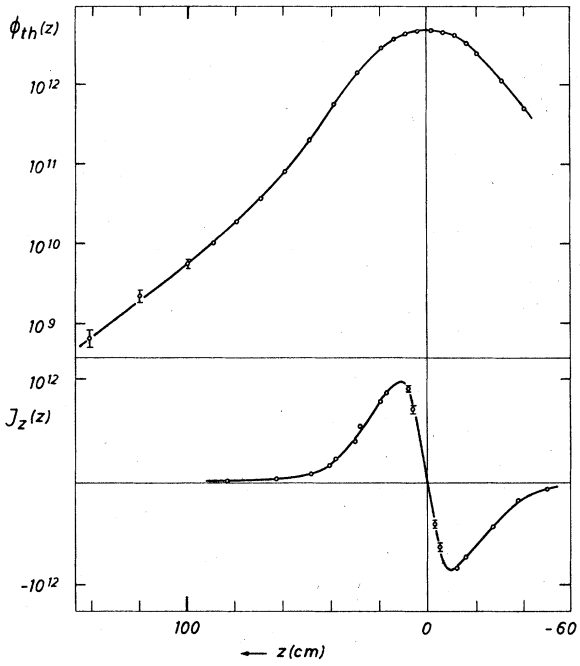

FIG. 2. Thermal-neutron flux density $\Phi_{th}(z)$ and z component of the thermal-neutron current density $J_z(z)$ in the core-near region.

increases by an average of $\bar{q}_z = (7.50 \pm 1.36) \times 10^{-5} m_e c$. According to Ref. 26 one has to multiply the measured spectrum $N(p)$ by a correction factor

$$K_A(p) = 1 - [\bar{q}_z dN(p)/dp]/N(p). \quad (7)$$

B. Beam tube

1. Vacuum system

The mean pressure in the neutron-decay apparatus has to be small enough to allow an energy-independent transmission of the proton spectrum. The first measurement of the composition of residual gases released in an aluminum chamber by reactor radiation was reported by Baltacis *et al.*[27] On this basis, Paul and Nachtmann[28] calculated the maximum admissible pressure to be 3.5×10^{-8} torr (4.6×10^{-6} Pa). Although the outgassing data as well as the cross sections used in this estimate were not known with sufficient accuracy, it turned out that this guess was a rather good basis for the design of the beam tube (see Sec. IV B 4). The vacuum system satisfying this condition has been described in detail in Ref. 24. In addition to the standard oil-free UHV system outside the biological shield, a chemical getter pump (SORB-AC PUMP, SAES-Getters, Milan, Italy) had to be installed in the beam tube close to the proton source, because of the low conductances caused by the collimators and shieldings. For outgassing, the beam tube can be heated up to roughly 100°C by a closed water loop. The same loop is used for cooling during the measurement periods.

According to Ref. 24, the pressure averaged from the spectrometer to the decay proton source, $\bar{p}_{sc}$, can be estimated from the pumping speeds and conductances as

$$\bar{p}_{sc} = p_s + 11\Delta p_s + 0.001 p_r, \quad (8)$$

where p_s is the pressure at the spectrometer, p_r is the pressure at the reference proton source (both measured with the reactor shut down), and Δp_s is the increase of pressure obtained at the spectrometer owing to reactor operation. Typical values are given in Table III. Since some of the values of $\bar{p}_{sc}$ were not negligible, an experimental correction was applied (see Sec. IV B 4).

TABLE III. Typical values of total pressure in the neutron decay apparatus.

No.	p_s (Pa)	p_r (Pa)	Δp_s (Pa)	$\bar{p}_{sc}$ (Pa)
1	1.5×10^{-7}	1×10^{-5}	4.4×10^{-7}	4.9×10^{-6}
2	9.0×10^{-8}	5×10^{-6}	1.6×10^{-7}	1.9×10^{-6}
3	1.6×10^{-6}	2×10^{-5}	1.3×10^{-6}	1.6×10^{-5}

2. Disturbing electric and magnetic fields

Electric disturbing fields (owing to charging of the inside walls by secondary electrons from the reactor γ radiation) have to be expected. This charging effect strongly depends on the wall material. Furthermore, secondary electrons cause a space charge inside the vacuum system.

The magnetic field inside the beam tube is due to the earth's field and due to remanent fields from the reactor structure. Before installing the (magnetically double shielded) apparatus into the beam tube, we measured a longitudinal component $H_z \cong 160$ m0e, and transverse components $H_x \cong 60$ m0e and $H_y \cong 160$ m0e (Kerschbaum[29]).

Magnetic and electric fields may influence the measured shape of the proton spectrum in three different ways:

(1) Transverse magnetic and electric fields shift the "effective source volume" (i.e., the source volume as "seen" by the spectrometer) and—owing to the variation of the source density in the x and y direction—thus change the decay proton intensity in an energy-dependent way.

(2) The negative space charge in the source volume retards the protons by an amount depending on their point of origin. Furthermore, the corresponding radial and longitudinal electric fields may give rise to unwanted focusing effects on the protons, depending on their energy and point of origin.

(3) Transverse magnetic and electric fields cause an erroneous energy calibration: By the influence of these fields the angle of incidence at the entrance of the spectrometer will be different for the decay protons and for those from the reference proton source.

The disturbing effects mentioned in points (1) and (2) have been theoretically treated by Paul and Nachtmann.[28] According to their study, the tolerable field limits are closely connected to the transverse gradients of the decay source. Their estimate took into account that the fields are larger in the core region owing to the decreasing permeability of the magnetic shield. They obtained the following maximum tolerable values:

$$E_x = 4.6 \text{ mV/cm}, \quad H_y = 25 \text{ m0e}$$

(in the core region) and

$$E_x = 1 \text{ mV/cm}, \quad H_y = 5.8 \text{ m0e}$$

(in the collimator region). The longitudinal component of the magnetic field, H_z, is limited to 160 m0e. For the acceptable depth of the electric

potential (i.e., the difference between the center and the wall of the tube) they gave $|V| \leq 0.1$ V.

The error in the energy-scale calibration, point (3), limits (for the case of homogeneous fields) the transverse components of the electric and magnetic fields to $E_x = 0.34$ mV/cm and $H_y = 2.0$ m0e.

3. Measures to reduce electric fields

The estimates of Paul and Nachtmann[28] yield for a reactor power of 7 MW and a dose rate $D_{\gamma 0} = 3.9 \times 10^7$ R/h (0.11 W/g) a secondary electron density $n^- = 330/\text{cm}^3$.

The assumption of a constant space-charge density $\rho = -n^- e$ in the core-near region of the cylindrical vacuum tube ($R = 4.5$ cm) leads to a parabolic potential distribution

$$V(r) = \rho(R^2 - r^2)/4\epsilon_0 . \tag{9}$$

One obtains $V_{\max} = -3.4$ mV at the axis ($r = 0$) and $E_{\max} = -1.0$ mV/cm at a radius $r = 3$ cm, which corresponds to the boundary of the decay-proton source. Thus the condition for the potential depth is easily fulfilled, while the field strength is close to the limit.

The charging effect of surfaces due to electron bombardment was investigated in a separate study (Ref. 30; for a short summary see Ref. 24), since a measurement *in situ* turned out to be impracticable. It was found that, after coating with colloidal graphite, the change in surface potential on aluminum samples was sufficiently low. Therefore, all inner surfaces seen by the decay protons (mainly the inside wall of the aluminum vacuum chamber and the chromium-plated copper collimators) were coated by spraying a colloidal graphite solution. As an additional measure an oil-free pumping system was employed. From the surface potential study quoted and the measured gradients of the γ radiation, the electrical field was estimated to be less than 1 mV/cm.

4. Measures to reduce the magnetic field

The earth's magnetic field was reduced by a double layer of Mumetal (see Refs. 24, 29, 31). The shielding consists of coaxial tubes with 30 cm length, mutually overlapping at the joints. This double-layer system is situated outside the vacuum system in order to avoid additional outgassing in the vacuum. It is surrounded by the heating (respectively, cooling) system of the overall beam tube insert. At the ends of the beam tube the shield overlaps with Mumetal tubes inside the vacuum system. When the system was put together inside the reactor beam tube for the first time, transverse fields between 0.1 and 0.2 m0e and an average longitudinal field of about 15 m0e were measured. The residual field in the spectrometer (shielded in a similar way) amounted to 1.5 m0e. The magnetic field measurement was repeated after three years of operation in site. At that time the transverse field amounted to about 20 m0e near the core, and the average value between the first collimator and the spectrometer entrance was less than 2 m0e. With regard to point (3) (Sec. III B 2) calculations based on the measured field showed that, owing to partial cancellation of the field influence, this effect is very small. Therefore its estimated value was added absolutely to the errors quoted below.

C. Spherical condenser spectrometer

A 90° spherical condenser spectrometer was used with a mean radius of 30 cm and an electrode distance of 6.0 cm. The entrance aperture (at position z_2) is circular with a diameter of 3.8 cm. The exit aperture is a rectangle with a width of 1.4 cm. According to calculations of Kubischta,[32] the energy dispersion is $D = 33.3$ cm, and the size of the image of the object at position z_1 (with diameter $G' = 4.0$ cm) is $G'' = 0.53$ cm. With these figures, the intrinsic resolution $R = G''/D$ amounts to 1.59%. The exact calculation of the various particle paths through the spectrometer—taking the finite size of the object at z_1 into account—yields an image (narrowest cross section of the beam) with a certain intensity distribution in the horizontal plane. If one compares the first moment of this distribution with the first moment of a point source in the center of the object, there is a shift of 0.14% towards lower energies for the extended source. As the energy calibration was done with the reference proton source—corresponding very closely to a point source—the energy calibration has to be corrected for this effect ("extended source correction").

Owing to the finite width of the spectrometer exit aperture (1.4 cm), the actual resolution is 4.2% and the resolution curve is of trapezoidal form. The probability to measure a particle with "true" energy T' at an energy setting of the spectrometer corresponding to a "measured" energy T depends only on T/T'. This probability distribution is called response function $F(T/T')$. The spectrum of counting rates $n(T)$ can therefore be obtained by folding the original spectrum $N(T')$ with the response function,

$$n(T) = \int_0^\infty N(T')F(T/T')dT' . \tag{10}$$

The width of the resolution function was experimentally determined to (4.20± 0.01)% independent of proton energy.

D. Detector system

The aim of the design was to obtain a constant detection efficiency close to 100% and a low background counting rate. The principle of the system (ion-electron converter type) can be seen on Fig. 3. The protons enter from the left side leaving the spectrometer, and are accelerated by a lens system (electrodes A, B, C, and D) to about −25 kV. The accelerated protons hit a thin (20–40 $\mu g/cm^2$) Al foil which is inclined by 45° with respect to the proton flight path, and eject secondary electrons from both sides of the foil. These electrons are accelerated and focused by the two cylinder lenses E_1 and E_2 onto two thin scintillator foils (NE 102 A), mounted on glass windows. Two photomultipliers (RCA 8575) are optically coupled to these windows. Only coincident counts of the two detectors are accepted as proton events. The coincidence background at full power (7 MW) of the reactor amounted to approx. 0.1 counts/sec.

Several measures were taken to avoid a dependence of the counting efficiency on the proton energy selected in the spectrometer. The coefficient of secondary-electron emission varies with the energy of the incident protons. Therefore, the 25 kV acceleration voltage (electrode D) was regulated in such a way as to make the proton end energy at the Al foil independent of the primary proton energy. Because of this potential regulation it was necessary to vary also the potential of the electrodes E_1 and E_2 together with the scintillators (covered with an evaporated Al layer) accordingly in order to keep the electron energy at the scintillator constant, because of the energy dependent photon yield in the scintillators.

An optimum focusing of the protons on the Al foil was attained by varying the potential of electrode C between −2 and −5 kV according to a calculated and experimentally tested function of the selected proton energy (Benka,[33] Stratowa[34]).

The decay proton image on the foil was 3.5 mm (horizontal) times 1 mm. The diameter of the foils used was 10 mm. Within the thickness range chosen the foils discriminated effectively against heavy ions. Six foils could be employed by means of a rotatable disc without interrupting the vacuum cycle.

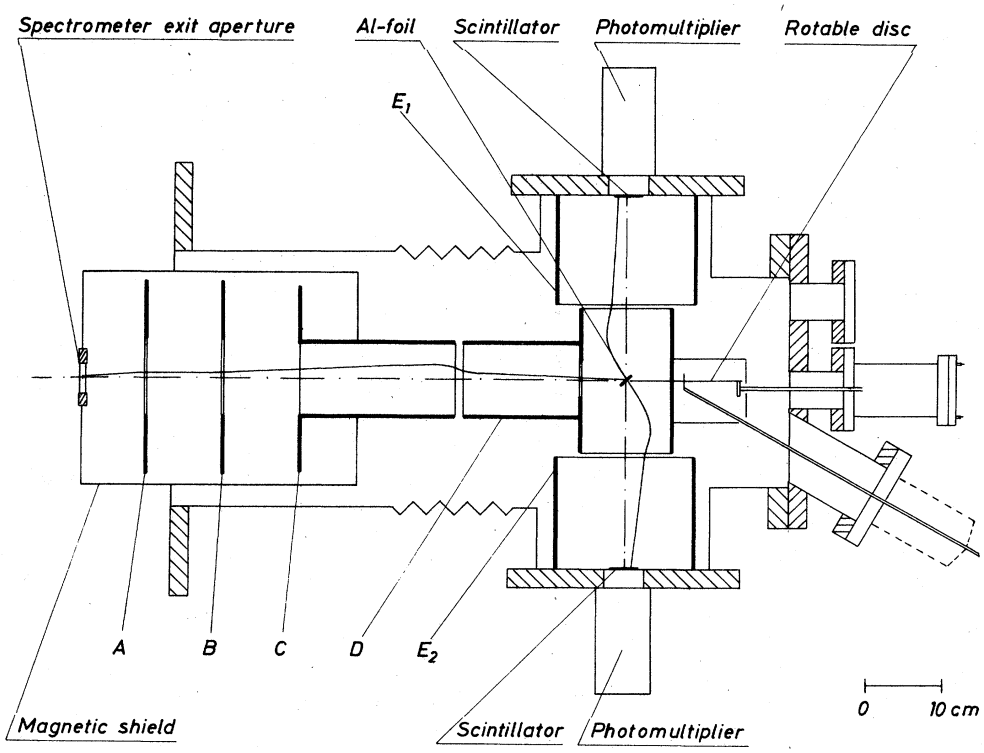

FIG. 3. Ion-electron converter detection system.

E. Reference proton source

The proton source used, a special version of an electron-impact ion source, employed ionization of hydrogen in a tantalum cage by three crossed electron beams. The extraction aperture had a diameter of 0.3 mm, the beam divergence was essentially determined by two apertures of 0.3 mm at a distance of 17.5 cm. A small and well defined divergence of the beam was necessary, because the ion-beam cross section must be smaller than the entrance aperture of the spectrometer after a drift distance of 7.5 m. A precisely defined average energy is most important since the energy calibration has to be done absolutely by this source and has a critical influence on the accuracy of the a value. In the ion source two effects influence the true energy of the ion beam:

(a) the space charge of the three electron beams and the transconductance of the acceleration field,

(b) the difference in the work functions on the cage surface and on the spherical condenser.

These corrections consist of a constant and an energy-dependent term and amount, e.g., to -0.8 eV at 500 eV energy. Finally, our energy calibration had a remaining error of 5×10^{-4}, the energy width was 2×10^{-3} or less.

The beam intensity was to be kept constant within 1%. This was required in order to measure the detection efficiency of the various Al foils and their local homogeneity. For checking the mass discrimination of the foils a beam chopper was installed at the ion source, and the ion mass could be determined by time-of-flight technique.

IV. RESULTS

A. Energy spectrum

In the middle part of Fig. 4, the energy spectrum $N(T)$ is shown for the values $a=0$ and $a=-0.1$. The sensitivity $S=[N(T)_{a=-0.1}/N(T)_{a=0}-1]\times100$ of the spectrum with regard to a is given in the lower part of this figure. The upper part shows the actual counting rates $n(T)$ taking the fact into account that the energy interval measured is proportional to the energy T.

A measurement at equal energy steps through the spectrum $n(T)$ yields very low counting rates near the lower and the upper end of the spectrum. A choice of the energy values as shown in Fig. 4 gives a better statistical information during a given measuring time. The measured points and their errors in this figure are taken from a typical spectrum (20 hours measuring time). The background counting rate was determined after each single scan (200 sec/point) at 0 eV and 775 eV.

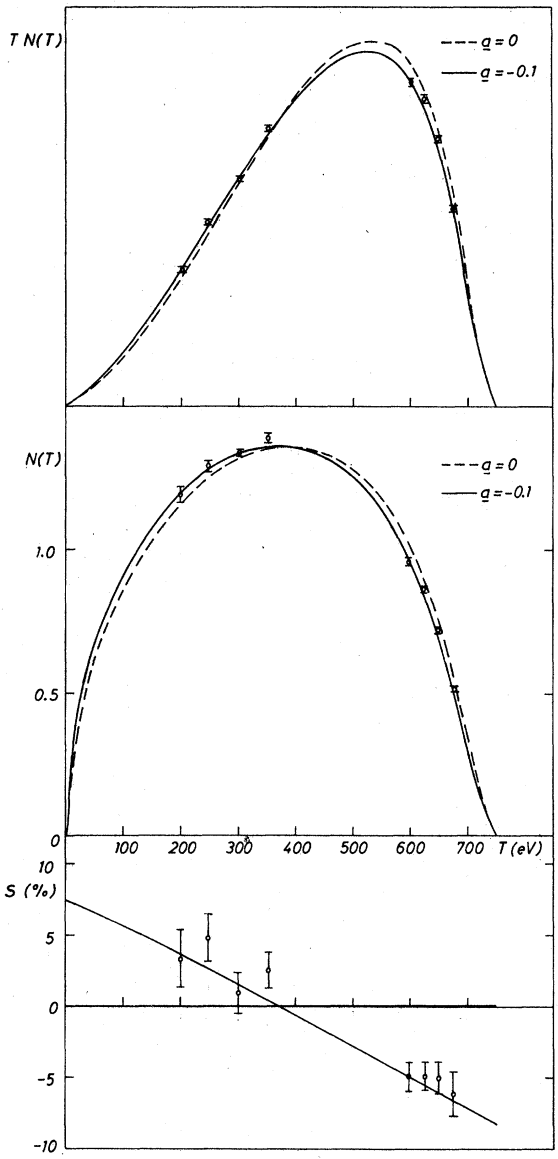

FIG. 4. Proton counting-rate spectrum, energy spectrum, and spectrum normalized to the spectrum for $a=0$ together with experimental points (20-h run).

Actually 35 spectra of this type were measured, most of them during a 24-h run. A very detailed account of the measurements and the calibration procedures is given in Ref. 34.

B. Evaluation

The evaluation proceeded in the following way: First the theoretical energy spectrum $N(T)$, see Eq. (3), was multiplied by the respective energy value T in order to obtain the theoretical counting rate spectrum $n(T)$. In the next step, the energy scale was changed with respect to the deviation

of the true energy of the reference proton source and to the extended source correction. Then the corrections (except the radiative corrections) are applied to the theoretical counting-rate spectrum by multiplying it with the corresponding functions $K_i(T)$. After applying these corrections to the theoretical counting-rate spectrum $n(T)$ we performed a least-squares fit to the experimental points by varying the parameter a. From this a preliminary value for $|\lambda|$ was calculated and then the radiative corrections were applied.

1. Energy-calibration corrections

These corrections are the following:

Uncertainty of the correction for true reference proton energy: ±0.05% in T,

Correction for extended source of decay protons: $K_E(T) = 1.0014 \pm 0.0005$.

2. Resolution correction

This correction was calculated by Nachtmann and Paul.[26] The correction factor $K_R(T)$ for the actual trapezoidal response function $F(T/T')$ with a width (full width at half height) of 4.2% is shown in Fig. 5.

3. Correction for the thermal motion of the neutrons

The correction factor $K_A(T)$ is the reciprocal of Eq. (7), but now calculated as function of T. It is shown in Fig. 6.

4. Vacuum correction

The influence of the residual gas on the proton spectrum measured was determined by comparing the decay proton spectrum at deliberately chosen moderate vacuum conditions (1.6×10^{-5} and 8.6×10^{-4} Pa) with that at optimum vacuum conditions. Figure 7 shows the correction factor $K_V(T)$ for an average pressure $\bar{p}_{sc}$ of 1.6×10^{-5} Pa. To each proton spectrum the correction function according to the actual pressure during the measurement was applied. The uncertainty of this correction was estimated to be ±10%.

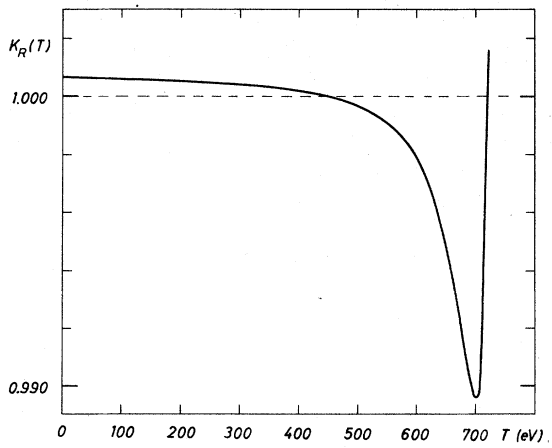

FIG. 5. Resolution correction for 4.2% energy width.

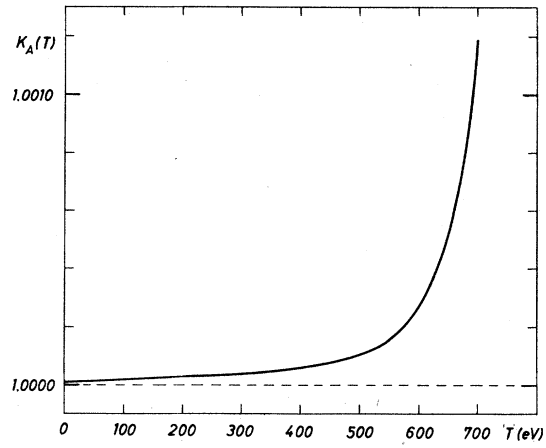

FIG. 6. Correction for 2.1% asymmetry in thermal-neutron flux.

5. Relativistic correction

A calculation of Nachtmann[22] showed that the influence of relativistic effects of nucleon motion on the value of a are smaller than 5×10^{-6}. This correction is neglected.

6. Scattering in the spectrometer

There is a possibility that protons of an energy different from the energy selected are scattered by the electrodes of the spectrometer and thus change the proton counting rate. Experimental

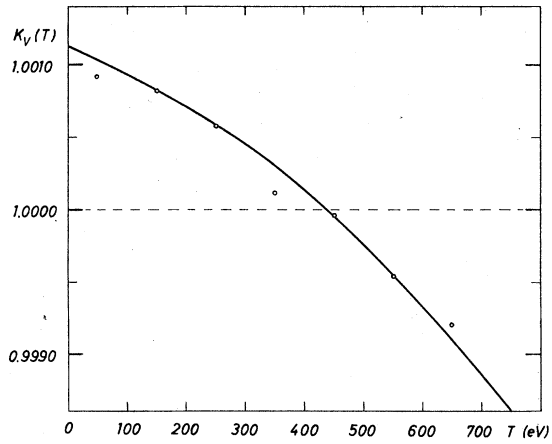

FIG. 7. Vacuum correction measured for a mean pressure $\bar{p}_{sc} = 1.6 \times 10^{-5}$ Pa.

tests using the reference proton source showed that this fraction of protons is smaller than 5×10^{-5}. The correction is neglected.

7. Radiative corrections

The radiative corrections to the proton recoil spectrum in neutron decay were calculated by Christian[35] and Christian and Kühnelt.[36] In this case the theoretical spectrum (corrected for radiative effects) depends on λ in the following form:

$$N(T)=g_V^2[A(T)+\lambda^2B(T)]. \tag{11}$$

$A(T)$ and $B(T)$ are listed in Ref. 35, they are quoted with an error of 10^{-3}. Therefore, first all other corrections were applied and the fit between theoretical spectrum and experimental points was carried out yielding a preliminary a value. From this one obtains $|\lambda|=1.272$. Now $N(T)$ may be calculated from Eq. (11); $K_S(T)$—see Fig. 8—is then obtained by taking $K_S(T)=N(T)/N_0(T)$, where $N_0(T)$ is the theoretical spectrum without the radiative corrections. The radiative corrections lower the value of $|\lambda|$ by about 1%.

8. Results

After applying all corrections quoted and averaging the results for a of the 35 measured spectra the results are

$$a=-0.1017\pm0.0019,$$

$$|\lambda|=|g_A/g_V|=1.259\pm0.006.$$

The errors quoted here are only statistical.

Taking into account the uncertainties of the corrections applied and of the calibration measurements, we calculated the possible systematic error. All contributions to the discussed corrections were quadratically added, giving a systematic error in a of ±0.0042. The estimate of the influence of the residual magnetic field and the uncertainty in the response function (together ±0.0005 in a) were added in absolute value. This way we obtain

$$a=-0.1017\pm0.0051,$$

$$|\lambda|=|g_A/g_V|=1.259\pm0.017.$$

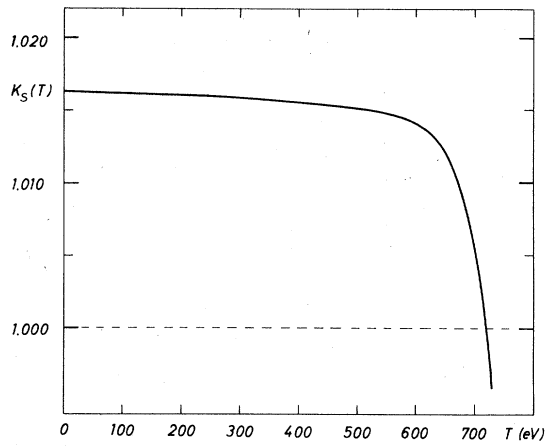

FIG. 8. Correction for radiative effects.

In order to characterize the quality of the result the fact was taken into account that the values of a obtained from each of the 35 spectrum measurements are quantities derived from counting rates. Thus it is possible to define an internal error of the mean value of a. The external error follows from the derivation of the individual values of a from the mean. This way the ratio R between external and internal error can be calculated and yielded 1.01. This excellent value of R is surprising for a series of measurements extended over a considerable length of time and with slight experimental modifications between taking data. It is therefore felt that the latter quoted errors might be too conservative and that the actual accuracy lies between the two errors quoted above.

V. ACKNOWLEDGMENTS

The contributions of Professor H. Paul, Dr. P. Riehs, and D. I. E. Kerschbaum in the earlier part of the work are thankfully acknowledged. The authors are further indebted to the staff of the ASTRA reactor led by Dr. A. Burtscher, to the personnel of the workshop led by D. I. Schindler, and to W. Pointner for their continuous support. This research was supported in part by the U. S. Government under Contracts Nos. 61(052)-857 and F61052-69-C-0038, and by the "Fonds zur Förderung der wissenschaftlichen Forschung in Österreich," Vienna.

[1]J. D. Jackson, S. B. Treiman, and H. W. Wyld, Jr., Phys. Rev. 106, 517 (1957).
[2]S. Raman, T. A. Walkiewicz, and H. Behrens, At. Data Nucl. Data Tables 16, 451 (1975).
[3]M. A. Clark and J. M. Robson, Can. J. Phys. 38, 693 (1960).
[4]M. A. Clark and J. M. Robson, Can. J. Phys. 39, 13 (1961).

[5]M. T. Burgy, V. E. Krohn, T. B. Novey, G. R. Ringo, and V. L. Telegdi, Phys. Rev. 120, 1829 (1960).
[6]C. J. Christensen, V. E. Krohn, and G. R. Ringo, Phys. Lett. 28B, 411 (1969).
[7]C. J. Christensen, V. E. Krohn, and G. R. Ringo, Phys. Rev. C 1, 1693 (1970).
[8]B. G. Erozolimsky, L. N. Bondarenko, Yu. A. Mostovoy, B. A. Obinyakov, V. A. Titov, V. P. Zacharova, and A. I. Frank, Phys. Lett. 33B, 351 (1970).
[9]B. G. Erozolimskii, L. N. Bondarenko, Yu. A. Mostovoi, B. A. Obinyakov, V. P. Zakharova, and V. A. Titov, Yad. Fiz. 11, 1049 (1970) [Sov. J. Nucl. Phys. 11, 583 (1970)].
[10]B. G. Erozolimskii, L. N. Bondarenko, Yu. A. Mostovoi, B. A. Obinyakov, V. I. Fedunin, and A. I. Frank, Zh. Eksp. Teor. Fiz. Pis'ma Red. 13, 356 (1971) [JETP Lett. 13, 252 (1971)].
[11]B. G. Erozolimskii, Yu. A. Mostovoi, V. I. Fedunin, and A. I. Frank, Zh. Eksp. Teor. Fiz. Pis'ma Red. 20, 745 (1974) [JETP Lett. 20, 345 (1974)].
[12]R. I. Steinberg, P. Liaud, B. Vignon, and V. W. Hughes, Phys. Rev. Lett. 33, 41 (1974).
[13]R. I. Steinberg, P. Liaud, B. Vignon, and V. W. Hughes, Phys. Rev. D 13, 2469 (1976).
[14]V. E. Krohn and G. R. Ringo, Phys. Lett. 55B, 175 (1975).
[15]B. G. Erozolimskii, A. I. Frank, Yu. A. Mostovoi, and S. S. Arzumanov, Zh. Eksp. Teor. Fiz. Pis'ma Red. 23, 720 (1976) [JETP Lett. 23, 663 (1976)].
[16]Yu. V. Trebukhovskii, V. V. Vladimirskii, V. K. Grigor'ev, and V. A. Ergakov, Zh. Eksp. Teor. Fiz. 36, 1314 (1969) [Sov. Phys.—JETP 9, 931 (1959)].
[17]V. V. Vladimirskii, V. K. Grigor'ev, V. A. Ergakov, D. P. Zharkov, and Yu. V. Trebukhovskii, Bull. Acad. Sci. USSR 25, 1128 (1968).
[18]V. K. Grigor'ev, A. P. Grishin, V. V. Vladimirskii, E. S. Nikolaevskii, and D. P. Zharkov, Yad. Fiz. 6, 329 (1967) [Sov. J. Nucl. Phys. 6, 239 (1968)].
[19]R. Dobrozemsky, E. Kerschbaum, G. Moraw, H. Paul, C. Stratowa, and P. Weinzierl, Phys. Rev. D 11, 510 (1975).
[20]O. Kofoed-Hansen, K. Dan. Vidensk. Selsk. Mat. Fys. Medd. 28, No. 9 (1954).
[21]P. Riehs, Acta Phys. Austriaca 27, 205 (1968).
[22]O. Nachtmann, Z. Phys. 215, 505 (1968).
[23]D. E. Kraus and F. A. White, IEEE Trans. Nucl. Sci., NS-13, 765 (1966).
[24]R. Dobrozemsky, Nucl. Instrum. Methods 118, 1 (1974).
[25]C. J. Christensen, A. Nielsen, A. Bahnsen, W. K. Brown, and B. M. Rustad, Phys. Rev. D 5, 1628 (1972).
[26]O. Nachtmann and H. Paul, Z. Phys. 226, 17 (1969).
[27]E. Baltacis, R. Dobrozemsky, and W. Kubischta, in *Proceedings of the 4th International Vacuum Congress, Manchester, 1968* (Institute of Physics and Physical Society, London, 1970), p. 767.
[28]H. Paul and O. Nachtmann, Ann. Phys. (Leipzig) 23, 397 (1969).
[29]E. Kerschbaum, Diplomarbeit, Univ. of Technology, Vienna, 1968 (unpublished).
[30]R. Dobrozemsky and E. Haltau, Dutch J. Vac. Tech- vol. 8, 133 (1970).
[31]R. Dobrozemsky, *Proceedings of the 3rd International Conference on Magnet Technology, Hamburg, 1970* (DESY, Hamburg, 1970), p. 1629.
[32]W. Kubischta, dissertation, Univ. of Technology, Vienna, 1968 (unpublished).
[33]O. Benka, dissertation, Univ. of Vienna, 1970 (unpublished).
[34]C. Stratowa, dissertation, Univ. of Vienna, 1977 (unpublished).
[35]R. Christian, dissertation, Univ. of Vienna, 1976 (unpublished).
[36]R. Christian and H. Kühnelt, Acta Phys. Austriaca 49, 229 (1978).